Journal of Statistical Physics, Vol. 80, Nos. 3/4, 1995

Description of Ordering and Phase Transitions in Terms of Local Connectivity: Proof of a Novel Type of Percolated State in the General Clock Model

Yohtaro Ueno[1]

Received July 3, 1993; final November 28, 1994

We present a new description of ordering and phase transitions in terms of genuine local connectivity, i.e., physical connections and disconnections which lead to global order and disorder, respectively. It is generally applicable to complex spin models. We apply it to a simple case of the d-dimensional Q-state general clock (GCL) model with two interaction energy parameters ($0 \leqslant \varepsilon_1 \leqslant \varepsilon_2$). This model was previously studied for $Q=6$ in $d=3$ by the Monte Carlo twist method. The following are the main results. There are novel types of ordered phases (called IOPs) which are ferromagnetic but dominated by two- or three-spin states and exhibit much softer behavior, with stiffness exponent $\psi \approx 1.2$, than the low-temperature ferromagnetic phase, with $\psi = 2$, and one of their phase transitions occurs without symmetry breaking. The physical connections and disconnections are expressed in terms of new variables, link (l-), hinge (h-), and vacant (v-) bonds. We introduce a new version of the GCL model with $\varepsilon_2 = \infty$ (called RGCL model) which cannot be disordered, since it has no v-bonds. It is proved to be equivalent to the restricted SOS model for $Q > 4$ in the hypercubic lattice. Then we prove that at least one percolated phase of h-bonds exists at high temperature (at any temperature for $\varepsilon_1 = 0$) in the d-dimensional RGCL model for $\infty > d > 1$. For the GCL model with $\varepsilon_1 = 0$ where $\varepsilon_2 < \infty$, we then prove the existence of it at low enough temperatures. Based on these results and from the numerical study mentioned above, we obtain that the IOPs are percolated states of h-bonds, and the phase transition without symmetry breaking is purely topological. Also, for the SOS models in $d > 2$ given by $\mathcal{H} = \sum |H_i - H_j|^k$, we show there is a boundary k_c (≈ 5) that separates them into two regimes, a preroughening transition for $k > k_c$ and no transitions otherwise. An algorithm for the GCL model and order parameters of these percolated phases are given in terms of clusters of l- and h-bonds. The IOPs are also discussed in detail.

[1] Department of Physics, Tokyo Institute of Technology, Oh-okayama, Meguro, Tokyo 152, Japan.

0022-4715/95/0800-0841$07.50/0

KEY WORDS: Local connectivity; bond variables; clusters; general clock model; SOS model, incompletely ordered phase; percolated state; topological phase transition; algorithm.

1. INTRODUCTION

One is used to considering ordering and phase transitions in terms of order parameters. Naturally one should have a naive idea that the long-range order is a state in which a local connection between constituents extends over all the system. Since one is familiar with the notion of force, it is natural to have such an idea, but it is difficult to answer what the connection really is in a general case. In an Ising ferromagnet, the parallel states of nearest-neighbor (NN) spins might be supposed to be connected, but they are not, as is well known.[1] Since this model at $T=\infty$ becomes equivalent to the random site percolation problem with concentration $p=1/2$, both parallel states are percolating in three dimensions because $p_c<0.5$ for any lattice.[1] Therefore one cannot describe phase transitions in terms of such geometrical connectivity. It is our first aim to define genuine local connections and disconnections in a general case (which lead to order and disorder, respectively) and formulate the description of phase transitions in terms of them. We shall call these genuine quantities *physical connections* and *disconnections*.

Since the long-range order is brought about by the physical connections, the description based on local connectivity should be expected to give new and deeper insight into ordering and phase transitions. As a matter of fact, there has been great progress for the ferromagnetic Potts model. This approach led to a new percolation model, the so-called random cluster model[2] (or correlated bond percolation model[3]). Further making use of the transformation between two models led to the so-called Swendsen–Wang algorithm.[4] Since the algorithm accelerates the equilibration enormously, it has advanced not only the study of the static properties of phase transitions, but also that of critical dynamics.[3–6] However, the concepts of physical connection and disconnection have been defined only implicitly in the studies done so far. Thus one cannot generalize them to complex models with interaction energy parameters more than one. The present approach from local connective force to long-range order is shown to be indispensable to the description of nontrivial intermediate phases which can be expected in such complex models. It leads to the proof that such ordered phases are a novel type of percolated state.

In complex systems, there are some cases in which it is difficult to find order parameters and further even to identify phase transitions themselves. There has been great interest in them. Many such systems are seen in three

dimensions, such as the antiferromagnetic (AF) Potts model,[7–9] the stacked triangular AF Ising model,[10,11] the six-state general clock (GCL) model,[12,13] and so on.[14] The Q-state GCL model which we consider in the present paper becomes, by changing interaction parameters, the ferromagnetic Potts model, the ordinary clock model, and even a highly degenerate model which is considered equivalent to the three-state AF Potts model for $Q=6$.[12] A series of studies of three-dimensional (3D) models by the Monte Carlo (MC) twist method[8,12,13,16] have revealed a novel type of ordered phase (called incompletely-ordered phases, IOP).[8,11–13] In the $Q=6$ GCL model,[13] they are ferromagnetic but are dominated by two- or three-spin states (which are adjacent to each other) and are soft in stiffness, whereas the ordinary ferromagnetic phase is dominated by a single-spin state and is rigid. Thus the latter is called the completely ordered state (COP). It is striking that one of the phase transitions of the IOPs is not accompanied by symmetry breaking. It has been conjectured that the IOPs are a novel type of percolated state and the phase transition of interest is characterized only by percolation, i.e., is purely topological.

It is our additional purpose to verify the conjectures[13] on the 3D $Q=6$ GCL model mentioned above, on the basis of our description where physical connections and disconnections are represented by bond variables which are newly introduced. The verification is attained through some proofs on a new version of the GCL model which cannot be disordered. It turns out that the percolated phases are described only by kinds of bond variables which are hidden variables, as its percolation.

The paper is organized as follows. In Section 2, introducing the Q-state GCL model, we briefly review the properties of IOPs and their phase transitions for $Q=6$ in $d=3$ obtained by the MC twist method. In Section 3 we first define the physical connections and disconnections in the GCL model and describe the partition function in terms of them, introducing bond variables, and further in terms of their clusters. In Section 4 we introduce a restricted GCL model and prove that there exists at least one percolated state of a novel type in it, based on the preceding theorem (which is also proved there). In Section 5 we prove that such a percolated state survives in a certain low-temperature range at a special point of the energy parameters of the GCL model. In Section 6 we verify the conjectures previously made on the 3D $Q=6$ GCL model on the basis of the theorem in Section 5 and the MC study. We also obtain some properties of the SOS models by making use of its equivalence with the GCL model in a limit. In Sections 7 and 8 the order parameters of the percolated states and algorithm are given in terms of clusters. We give some comments on related models and detailed discussions on the IOPs in Sections 9 and 10, respectively. The final section is devoted to a summary.

2. THE GCL MODEL AND THE MONTE CARLO RESULTS

We define the Q-state GCL model[15] on a d-dimensional hypercubic lattice which is built up out of edges and sites where a spin σ lies at each site. We assume the lattice is isotropic with free boundary conditions and has N sites. The spin variable σ_i at the ith site takes Q different states labeled by $1, 2, \ldots, Q$ which are associated with the clock angles by $\theta_i = 2\pi\sigma_i/Q$. We consider only the models with nearest-neighbor (NN) interactions and no external field. The spins interact with their NNs, depending on their relative angle $|\theta_i - \theta_j|$ with mod 2π, thus $\sigma_{ij} = |\sigma_i - \sigma_j|$ with mod Q, which is defined by

$$V(\sigma_{ij}) = \sum_{m=0}^{[Q/2]} \varepsilon_m \delta(\sigma_{ij}, m) \tag{2.1}$$

where $\delta(\sigma, m)$ is the Kronecker delta function. Here, since σ_{ij} takes $[Q/2]+1$ independent states, where $[Q/2]$ is the Gauss notation, we have limited σ_{ij} in the range from 0 to $[Q/2]$:

$$\sum_{m=0}^{[Q/2]} \delta(\sigma_{ij}, m) = 1 \tag{2.2}$$

Then one has $[Q/2]$ independent energy parameters ε_m, setting $\varepsilon_0 = 0$. One has $\varepsilon_m \propto 1 - \cos(2\pi m/Q)$ for the ordinary clock model.

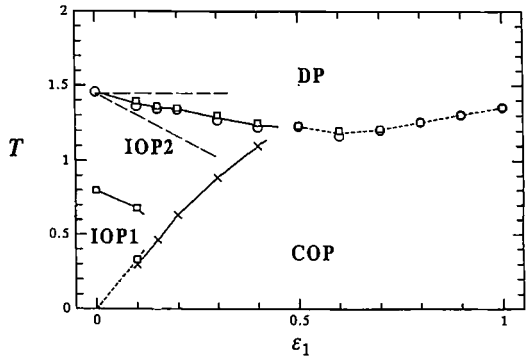

Fig. 1. Phase diagram of the 3D $Q=6$ GCL model with $\varepsilon_2 = 1.0$, obtained by the MC twist method; DP, COP, and IOP stand for disordered, completely ordered, and incompletely ordered phases, respectively. Solid and dotted curves indicate the second and first order transitions, respectively. Broken lines are $T = 1/\log 2$ and $T = (1-\varepsilon_1)/\log 2$, which are obtained from $p_0/p_v = 1$ and $p_1/p_v = 1$, respectively; these are explained in Section 6. See the text and ref. 13 for details, except for the broken lines.

Applying the Monte Carlo twist method, Ueno and Kasono studied a simple case of the $Q=6$ GCL model in which $\varepsilon_2=\varepsilon_3=1$ and $0<\varepsilon_1<1$, on the simple cubic lattice. We review it briefly; see ref. 13 for details. Figure 1 shows the phase diagram. In $0.5<\varepsilon_1\leqslant 1$, there is a coexistence line between the COP and the disordered phase (DP), as expected, since $\varepsilon_1=1$ is the ferromagnetic Potts model. Two kinds of IOPs exist at and near $\varepsilon_1=0$. Two-spin states are dominant in the IOP1, three states in the IOP2, as shown in Fig. 2. Since these dominant states are adjacent to each other, both the IOPs are ferromagnetic. As seen from Fig. 2, the IOP2 does not differ in uniform symmetry from the COP. Thus the phase transition between these phases is not accompanied by symmetry breaking.

In spite of being ferromagnetic, both the IOPs exhibit a large qualitative difference in stiffness when compared with the COP. To see this, it is most effective to use the stiffness exponent $\psi(T)$, which is defined as follows in the stiffness free energy, which is the increment of the total free energy when twisted by imposing appropriate boundary conditions:

$$\Delta F_L(T)=A(T)\,L^{\psi(T)} \tag{2.3}$$

for $L\to\infty$. The $\psi(T)$ represents not only a measure of stiffness of the long-range order, but also determines the critical point or line by $\psi(T)=0$ from the data of the system of finite sizes; note that $\psi<0$ indicates disorder. The COP is as rigid as $\psi=2$, which is attributed to interfaces, whereas both the IOPs are as soft as $\psi\simeq 1.2$. However, the IOP1 depends on the twist angle ϕ; $\psi\simeq 1.2$ for $\phi>\pi/3$ and $\psi<0$ at $\phi=\pi/3$, distinguishing it from the IOP2.

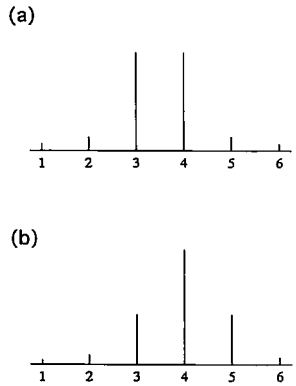

Fig. 2. Illustration of one-spin distribution function (probably vs. clock state) of (a) the IOP1 and (b) the IOP2, in the same model as in Fig. 1, obtained by the Monte Carlo twist method (after ref. 13).

The disorder-like behavior at $\phi = \pi/3$ indicates that the IOP1 is dominated by two adjacent spin states.

It is quite interesting to look at spin configurations in the IOPs. Figure 3 shows them in a cross section. Although the clusters are geometrical there, they are obviously percolated in the IOP1, but it does not appear that clusters in two subdominant spin states are percolated in the IOP2, though there might be a possibly of the percolation in the 3D space. It has been suggested that the COP–IOP2 transition is of second order and the possibility of first order is considered least probable. Then, assuming the second-order transition, Ueno and Kasono conjectured for the IOP2 that the clusters in the subdominant states should percolate in the system, by considering that it is the only possible behavior that gives a macroscopic difference between these phases. Because of the reason mentioned in Section 1, the percolated clusters that have been conjectured should be physical ones.

Finally, we generally define the COP and IOPs for the regular ferromagnetic models with discrete symmetry. The COP is the ordered phase that has $\psi = d - 1 > 0$ and is dominated only by a single spin state. Probably the former condition includes the latter. We assume there are no

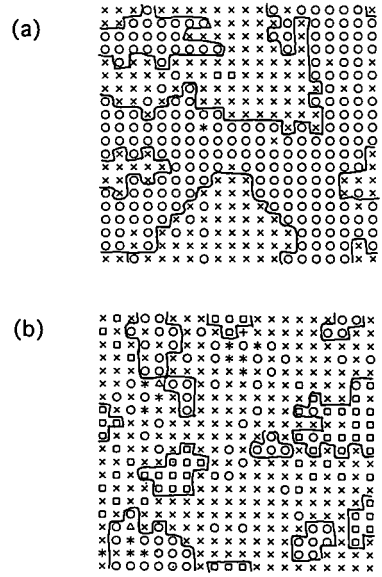

Fig. 3. Spin configurations in a cross section of (a) the IOP1 at $T = 0.55$ and (b) IOP2 at $T = 1.2$, in the $Q = 6$ GCL model with $\varepsilon_1 = 0.1$, $\varepsilon_2 = 1$, obtained by MC simulations. See ref. 13 for details.

ordered phases in which plural spin states are dominant in spite of $\psi = d-1$. We define that the IOPs are those phases which have $0 \leqslant \psi < d-1$ and $\psi \neq d-2$ and are dominated by plural spin states. In the regular AF models where no spins are competing, the COP is characterized, together with $\psi = d-1$, by a single Fourier component of the spin moment.

3. FORMULATION

3.1. Physical Disconnections and Connections

We consider the physical disconnections and connections in the Q-state GCL model, since it contains many models. Our interest is in the models that have more than one kind of physical connections, that is, energy parameters more than two, so that the models are limited to $Q > 3$. For simplicity we mainly consider below a simple case of this model where $0 < \varepsilon_1 < \varepsilon_2$ and $\varepsilon_m = \varepsilon_2$ for $m \geqslant 2$. Using Eq. (2.1), let us express the Boltzmann factor for $V(\sigma)$ in the following way.

$$e^{-\beta V(\sigma)} = \delta(\sigma, 0) + e^{-K_1}\delta(\sigma, 1) + e^{-K_2} \sum_{m=2}^{[Q/2]} \delta(\sigma, m) \tag{3.1a}$$

$$= A\{p_l \delta(\sigma, 0) + p_h \delta(\sigma, 1) + p_v\} \tag{3.1b}$$

where $\beta = 1/T$, $K_m = \beta\varepsilon_m > 0$ in units of $k_B = 1$, and

$$Ap_l = 1 - e^{-K_2}, \qquad Ap_h = e^{-K_1} - e^{-K_2}, \qquad Ap_v = e^{-K_2} \tag{3.2}$$

Here A is the normalization constant to satisfy $p_l + p_h + p_v = 1$. Note $p_l \geqslant p_h$ in the present study.

For a given spin configuration $\tilde{\sigma} = \{\sigma_i\}$ let us expand the Boltzmann measure

$$\mu(\tilde{\sigma}) = \prod_{\langle ij \rangle} \exp[-\beta V(\sigma_{ij})]/Z \tag{3.3}$$

with respect to the three terms in Eq. (3.1b), where $\langle ij \rangle$ represents a pair of NN sites and $Z = \sum_{\tilde{\sigma}} \prod_{\langle ij \rangle} \exp[-\beta V(\sigma_{ij})]$ is the partition function. It is convenient to regard these terms as new variables, calling them bond variables (the definitions will soon be given) and to put one of them with the corresponding probability on each edge of the lattice. Then $\mu(\tilde{\sigma})$ may be expressed by a series of graphs made up of these bonds.

Since $p_v = p_v \sum_{m=0}^{[Q/2]} \delta(\sigma, m)$, the bond for the last term in the curly brackets in Eq. (3.1b) occurs with equal probability p_v for any NN relative pair-spin state σ_{ij}. Therefore this bond makes no difference among all the

states of σ_{ij}, hence among the NN spin states (σ_i, σ_j). Therefore this kind of bond does not lead to any order and thus represents disconnection between neighboring spins. We call them *vacant bonds* henceforth.

Since the other kinds of bonds make differences among the NN relative pair-spin states, they represent physical connections. One is a link to form a cluster in the same spin state which occurs with probability p_l. We call it a *link bond*. The second connects, with probability p_h, two clusters in adjacent states; thus this kind of bond extends, producing surfaces. Since the last plays a role like a hinge connecting two clusters with the limited angles, we call it a *hinge bond*. We should remark that the link and hinge bonds exchange their roles in case of $\varepsilon_1 < 0 < \varepsilon_m$ $(m \geqslant 2)$.

The above definitions can be easily applied to other models. This is the basic idea that enables one to describe ordered phases and phase transitions in terms of local connectivity.

3.2. Description in Terms of Bond Variables

To make the above expansion in an explicit form it is convenient to introduce the bond variables[4,5] n_{ij}, which take three states, denoted by $\{l, h, v\}$ for {link, hinge, vacancy}, respectively. These bond states correspond to the above three terms in Eq. (3.1b). Henceforth we label these states simply by $n_{ij} = l, h, v$ and use the abbreviations l-, h-, v-bonds for them. Denoting by $\tilde{n} = \{n_{ij}\}$ a graph made up of three kinds of bonds given $\tilde{\sigma}$, one then gets

$$\begin{aligned}\mu(\tilde{\sigma}) &= \sum_{\tilde{n}} \mu(\tilde{n}; \tilde{\sigma}) \\ &= \frac{A^E}{Z} \sum_{\tilde{n}} \prod_{\langle ij \rangle} \{ p_l \delta(\sigma_{ij}, 0)\, \Delta(n_{ij}, l) \\ &\quad + p_h \delta(\sigma_{ij}, 1)\, \Delta(n_{ij}, h) + p_v \Delta(n_{ij}, v) \}\end{aligned} \tag{3.4}$$

where E is the number of edges in the lattice and

$$\Delta(n_{ij}, \alpha) = \begin{cases} 1 & \text{for} \quad n_{ij} = \alpha \\ 0 & \text{otherwise} \end{cases} \tag{3.5}$$

with $\alpha = l, h, v$. Here $\{\tilde{n}\}$ in $\mu(\tilde{n}; \tilde{\sigma})$ are restricted only to those compatible to $\tilde{\sigma}$.

We expand Eq. (3.4) first with respect to $\tilde{\sigma}$, dividing the lattice graph $\mathscr{L}$ into three parts: $\mathscr{L}_0(\tilde{\sigma})$, where $\delta(\sigma_{ij}, 0) = 1$; $\mathscr{L}_1(\tilde{\sigma})$, where $\delta(\sigma_{ij}, 1) = 1$;

and the rest $\mathscr{L}_c(\tilde{\sigma})$ $(=\mathscr{L}-\mathscr{L}_0-\mathscr{L}_1)$. One can also divide $\tilde{n}$ into $\tilde{n}_0$ in $\mathscr{L}_0$ and $\tilde{n}_1$ in $\mathscr{L}_1$. Then one gets

$$\mu(\tilde{n};\tilde{\sigma}) \propto \mu_0(\tilde{n}_0;\tilde{\sigma})\,\mu_1(\tilde{n}_1;\tilde{\sigma}) \prod_{\langle ij\rangle \in \mathscr{L}_c(\tilde{\sigma})} p_v \Delta(n_{ij}, v) \tag{3.6}$$

The definitions of μ_0 and μ_1 are given below, including the expressions expanded further with respect to $\tilde{n}$:

$$\begin{aligned}\mu_0(\tilde{n}_0;\tilde{\sigma}) &= \frac{1}{Z_0} \prod_{\langle ij\rangle \in \mathscr{L}_0(\tilde{\sigma})} (p_l \Delta(n_{ij}, l) + p_v \Delta(n_{ij}, v)) \\ &= \frac{1}{Z_0} p_v^{E_0(\tilde{\sigma})} \left(\frac{p_l}{p_v}\right)^{B_l(\tilde{n}_0)}\end{aligned} \tag{3.7}$$

[here $E_0(\tilde{\sigma})$ is the number of edges in $\mathscr{L}_0$ and B_l the number of l-bonds in $\tilde{n}_0(\tilde{\sigma})$]

$$\begin{aligned}\mu_1(\tilde{n}_1;\tilde{\sigma}) &= \frac{1}{Z_1} \prod_{\langle ij\rangle \in \mathscr{L}_1(\tilde{\sigma})} (p_h \Delta(n_{ij}, h) + p_v \Delta(n_{ij}, v)) \\ &= \frac{1}{Z_1} p_v^{E_1(\tilde{\sigma})} \left(\frac{p_h}{p_v}\right)^{B_h(\tilde{n}_1)}\end{aligned} \tag{3.8}$$

Here $E_1(\tilde{\sigma})$ is the number of edges in $\mathscr{L}_1$ and B_h the number of h-bonds in $\tilde{n}_1(\tilde{\sigma})$. The Z_0, Z_1 are appropriate normalization constants. The edges of $\mathscr{L}$ are decomposed as

$$E = E_0(\tilde{\sigma}) + E_1(\tilde{\sigma}) + E_c(\tilde{\sigma}) = B_l(\tilde{n}_0) + B_h(\tilde{n}_1) + B_v(\tilde{n})$$

where E_c is the number of edges in $\mathscr{L}_c$ and B_v is the total number of v-bonds in $\tilde{n}(\tilde{\sigma})$.

Eventually Eq. (3.6) can be simply written as

$$\mu(\tilde{n};\tilde{\sigma}) = \frac{1}{Z} (Ap_l)^{B_l(\tilde{n}_0)} (Ap_h)^{B_h(\tilde{n}_1)} (Ap_v)^{B_v(\tilde{n})} \tag{3.9a}$$

$$= \frac{1}{Z_v} \left(\frac{p_l}{p_v}\right)^{B_l(\tilde{n}_0)} \left(\frac{p_h}{p_v}\right)^{B_h(\tilde{n}_1)} \tag{3.9b}$$

$$= \frac{1}{Z_l} \left(\frac{p_h}{p_l}\right)^{B_h(\tilde{n}_1)} \left(\frac{p_v}{p_l}\right)^{B_v(\tilde{n})} \tag{3.9c}$$

where $Z_\alpha = Z/(Ap_\alpha)^E$. For $p_h = 0$, where $\varepsilon_1 = 1$ (i.e., the Potts model), only the graphs $\tilde{n}$ with $E_1 = 0$ (hence $B_h = 0$) contribute to $\mu(\tilde{\sigma})$, leading to the random cluster model.[2] For $p_h > 0$ and close to p_l $(\gg p_v)$, graphs with larger B_h are strongly favored.

3.3. Description in Terms of Clusters

Let us first introduce two kinds of physical clusters that are connected only with one kind of bond: l-bond clusters and h-bond clusters. In the former, l-bonds in a cluster connect to each other by possessing only common sites. In the latter, however, since each cluster connects two l-bond clusters that are common to all the h-bonds in it, the bonds in a cluster possess a common site or are parallel to each other at the distance of the lattice constant (see Fig. 4).

It is useful to introduce new lattice graphs $\mathscr{L}_l(\tilde{n}_0)$, $\mathscr{L}_h(\tilde{n}_1)$, and $\mathscr{L}_v(\tilde{n})$ that consist of the edges occupied only by l-, h-, and v-bonds, respectively, for given $\tilde{\sigma}$. Let μ_l and ξ_h be the cluster graphs of the μth l-bond and ξth h-bond clusters, respectively. We assume these lattice and cluster graphs include the sites within them and at their boundaries. Then the lattice graphs are the sets of these clusters: $\mathscr{L}_l = \{\mu_l\}$, $\mathscr{L}_h = \{\xi_h\}$. Then the numbers of bonds are also given in terms of clusters as

$$\begin{aligned} B_l(\tilde{n}_0) &= \sum_{\mu \in \mathscr{L}_l} b_\mu(\mathscr{L}_l) \\ B_h(\tilde{n}_1) &= \sum_{\xi \in \mathscr{L}_h} b_\xi(\mathscr{L}_h) \end{aligned} \tag{3.10}$$

where $b_\mu(\mathscr{L}_l)$ is the number of l-bonds in the μth cluster and $b_\xi(\mathscr{L}_h)$ the number of h-bonds in the ξth cluster.

Next, we classify degrees of spin freedom from the viewpoint of clusters, noting that a spin is located at a site. The spins in each l-bond cluster are described as a cluster spin τ_μ. There are other spins that cannot

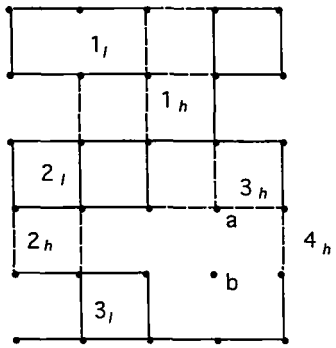

Fig. 4. Graph of a bond configuration in terms of clusters. Solid and broken lines are l- and h-bonds, respectively, while v-bonds are blank. There are three l-bond clusters and four h-bond clusters; the numbers denote these clusters. Sites a and b are one-site clusters where b is isolated.

be described by these cluster spins, i.e., their sites are shared in common only by h- and/or v-bonds as shown in Fig. 4. Since each spin on these sites behaves as an individual, we call them one-site cluster spins. Some of them interact with other cluster spins, whereas others are isolated and have only v-bonds. One-site clusters exist in $\mathscr{L}_{lc} = \mathscr{L} - \mathscr{L}_l$; here the boundary sites of $\mathscr{L}_l$ are not included. An isolated one-site cluster exists at every internal site of $\mathscr{L}_v$, that is, in $\mathscr{L}'_v = \mathscr{L}_v - \partial\mathscr{L}_v$, where $\partial\mathscr{L}_v$ represents the boundary sites of $\mathscr{L}_v$.

To express the partition function in terms of clusters, we first decompose the bond sum in Eq. (3.4) as

$$\sum_{\tilde{n}(\tilde{\sigma})} = \sum_{\mathscr{L}_l(\tilde{\sigma})} \sum_{\mathscr{L}_h(\tilde{\sigma})} \prod_{\langle ij\rangle \in \mathscr{L}_l} \sum_{n_{ij}} \Delta(n_{ij}, l) \times \prod_{\langle ij\rangle \in \mathscr{L}_h} \sum_{n_{ij}} \Delta(n_{ij}, h) \prod_{\langle ij\rangle \in \mathscr{L}_v} \sum_{n_{ij}} \Delta(n_{ij}, v) \tag{3.11}$$

Then we express the spin sum in terms of cluster spins τ_μ which include one-site cluster spins,

$$\sum_{\tilde{\sigma}} = \sum_{\mathscr{L}_l} \prod_{\mu \in \mathscr{L}_l} \sum_{\tau_\mu} \prod_{\mu \in \mathscr{L}_{lc}} \sum_{\tau_\mu} \tag{3.12}$$

A set of spin and bond configurations $(\tilde{\sigma}, \tilde{n})$ can be expressed by a set of a cluster configurations and cluster spins $(\mathscr{L}_l, \mathscr{L}_h; \tilde{\tau}_\mu)$, where $\tilde{\tau}_\mu$ includes one-site cluster spins, which is a one-to-one correspondence. Then, using Eqs. (3.9c), (3.11), and (3.12) and $\tau_{\mu\nu} = |\tau_\mu - \tau_\nu| \pmod{Q}$, one gets

$$\begin{aligned}
\sum_{\tilde{\sigma}} \sum_{\tilde{n}(\tilde{\sigma})} \mu(\tilde{n}; \tilde{\sigma}) &= \frac{1}{Z_l} \sum_{\mathscr{L}_l} \sum_{\mathscr{L}_h \subseteq \mathscr{L}_{lc}} \left(\frac{p_h}{p_l}\right)^{B_h(\mathscr{L}_h)} \left(\frac{p_v}{p_l}\right)^{B_v(\mathscr{L}_v)} \\
&\quad \times \prod_{\mu} \sum_{\tau_\mu} \prod_{\langle \mu\nu\rangle} \delta(\tau_{\mu\nu}, 1) \\
&= \frac{1}{Z_l} \sum_{\mathscr{L}_l} \sum_{\mathscr{L}_h \subseteq \mathscr{L}_{lc}} \prod_{\xi \in \mathscr{L}_h} \left(\frac{p_h}{p_l}\right)^{b_\xi(\mathscr{L}_h)} \left(\frac{p_v}{p_l}\right)^{B_v(\mathscr{L}_v)} Q^{N_{1s}(\mathscr{L}_v)} \\
&\quad \times \prod_{\mu \in \mathscr{L}'_{vc}} \sum_{\tau_\mu} \prod_{\langle \mu\nu\rangle}{}^{\mathrm{i}} \delta(\tau_{\mu\nu}, 1)
\end{aligned} \tag{3.13}$$

where $N_{1s}(\mathscr{L}_v)$ is the number of isolated one-site clusters in $\mathscr{L}'_v$, and $\mathscr{L}'_{vc} = \mathscr{L} - \mathscr{L}'_v$. Here $\prod^{\mathrm{i}}_{\langle\mu\nu\rangle}$ is the product over a neighboring pair of μth and νth l-bond clusters except the pairs that include isolated one-site clusters; the clusters in each pair are restricted to those directly connected by h-bonds.

3.4. Characterization of Disorder and Order

Some l-bond clusters and one-site clusters are surrounded only by v-bonds. The remaining ones form clusters of clusters connected by h-bonds, which we call *joint* clusters. Then each joint cluster is also surrounded only by v-bonds. All these clusters surrounded only by v-bonds are completely disconnected with each other, that is, isolated because the surrounding v-bonds do not prevent each of these clusters from taking any spin states independent of the other clusters.

From the definition of the physical disconnection, disorder is defined to be the state where only the v-bonds are dominant; that is, there are no infinite clusters of the l- and h-bonds. If isolated custers are finite, they can change their states with finite probabilities because the free energy barriers necessary for the changes are finite. Then it is obvious that long-range order is a state where at least one infinite cluster is present in thermal equilibrium.

To discuss the difference among percolated states, it is convenient to introduce colors which represent the spin states of clusters. The l-bond cluster μ_l takes Q states corresponding to the Q spin states $\tau_\mu = 1, 2, ..., Q$. We call these states colors of l-bond clusters, denoting them by $c(1)$, $c(2)$,..., $c(Q)$. Then the h-bond cluster can take the Q different colors intermediate between the corresponding pair of l-bond colors, which we denote by $c(12)$, $c(23)$,..., $c(Q1)$. Then the disorder is white, whereas the COP has one of $c(i)$ colors with tints of its neighboring $c(ii+1)$ colors, say, $c(2)$ with $c(12)$, $c(23)$, and so on. If there exist percolated phases of h-bonds, they are also characterized by both kinds of colors. If there could be a percolated state of h-bonds with two colors, say $c(12)$ and $c(23)$, which corresponds to the IOP2, then there might occur a phase transition between the COP and a percolated phase of h-bonds at which any color symmetries are not broken. These will be shown to exist and explained in Section 6.

4. PROOF OF PERCOLATED STATES IN THE RESTRICTED MODEL

4.1. Physically Connected Models

It is of considerable interest to consider those models in which no v-bonds can exist at any temperature, that is, $p_v = 0$. In the six-state GCL model one can get it by putting only $\varepsilon_3 = \infty$ or $\varepsilon_2 = \varepsilon_3 = \infty$. Then, as seen in Eqs. (3.7) and (3.8), thermal fluctuations cannot make any distribution of $\{\tilde{n}\}$ given $\tilde{\sigma}$. Thus $\tilde{n}$ is uniquely determined by $\tilde{\sigma}$, though the correspondence is one to many. Therefore two connections, physical and

geometrical, agree with each other. Since l- and h-bonds connect spins physically and any bond graphs consist only of them, these models exhibit only physically connected states, hence no disordered phase. Thus we may call them *physically connected* (PC) models. In general one can obtain known models of the PC type whose original models have interaction parameters more than one by lifting some of them to infinity, leaving at least one finite.

The solid-on-solid (SOS) models of crystal surfaces[17] are PC-type models. They are given by a single Hamiltonian,

$$\mathscr{H}_{\mathrm{SOS}} = \varepsilon_1 \sum_{\langle ij \rangle} |H_i - H_j|^k \tag{4.1}$$

where H_i is any integer. Here $k=1$ and 2 correspond to the absolute SOS and discrete Gaussian models, respectively. In Eq. (4.1) the largest energy parameter $\varepsilon_m = \varepsilon_1 m^k$ with $m = |H_i - H_j|$ diverges for $m \to \infty$. In case of $k=\infty$, only $m=0, 1$ are allowed, which is the restricted SOS (RSOS) model.[18]

In any SOS model the variable H_i is single-valued in the sense that the height at an arbitrary site does not change after a walk around along any closed path. Such singleness also exists in the present GCL model of PC type with $Q > Q_0$, which is obtained by putting $\varepsilon_2 = \varepsilon_3 = \infty$. Q_0 is equal to the number of sites on the elementary face of the lattice; thus $Q_0 \geqslant 3$ in general and $Q_0 = 4$ for the hypercubic lattice. Then the relative NN spin states are restricted only to $\sigma_{ij} = 0, 1$. Thus we call this model the *restricted* GCL (RGCL) model. In this model, height can be introduced as follows. Given $\tilde{\sigma}$, on an arbitrary path from one arbitrary site i to another site j, one defines the difference given by $\sigma_j - \sigma_i$ plus $m_{ij} = m_{ij}(Q \to 1) - m_{ij}(1 \to Q)$; here $m_{ij}(Q \to 1)$ and $m_{ij}(1 \to Q)$ are the times that σ_k changes from $\sigma_k = Q$ to 1 and from 1 to Q, respectively, when one proceeds all the way along the path. Since this is independent of the path, using this difference, one can transform σ_j to the height $H_j = \sigma_j + m_j Q$, where $m_j = m_{j0}$, assigning the height at the origin of sites to the origin of the height ($m_i = 0$ at $i=0$). However, for $Q \leqslant Q_0$ this singleness is broken because vortices can be generated. Thus we have the following theorem.

Theorem 1. The RGCL model with $Q > Q_0$ in $d > 1$ is equivalent to the RSOS model, where Q_0 is the number of sites on the elementary face of the lattice.

The singleness of the variables gives simple but crucial graphic features. In $d=2$, it requires that any connected line of h-bonds (or step contour) have no end, namely, be closed or terminate at the free boundaries of the system. In $d > 2$, a $(d-1)$-dimensional surface of h-bonds is

closed or percolated, both with no defect on the surface. This is also valid for all other SOS models, though one has to consider the surfaces made up of different kinds of h-bonds with various differences. The above statement is valid also for GCL models of PC type other than the RGCL model, so long as the singleness holds. Since only percolation of h-bonds can destroy the COP (or the flat phase), we immediately obtain the following theorem.

Theorem 2. There can exist only the COP and/or at least one h-bond percolated state in d-dimensional classical models of PC type with discrete single-valued variables for $d > 1$.

It is interesting to compare the present theorem with the established results of the SOS models in $d = 2$. As is well known, the SOS models undergo a roughening transition[17–19] between the rough and flat phases which is in the Kosterlitz–Thouless universality class.[20] It is obvious that all the step contours are closed in the flat phase, whereas some are percolated in the rough phase. In addition, the rough phase has the translational symmetry of the Hamiltonian (4.1), which is invariant for $\{H_i\} \to \{H_i + \Delta H\}$, where ΔH is an arbitrary height. Thus, it follows that step percolation of every color occurs in this phase.

4.2. Proof of h-Bond Percolated States in the RGCL Model

We prove the following theorem on the basis of Theorem 2.

Theorem 3. There exists the COP at $T \ll \varepsilon_1$ and at least one h-bond percolated state at $T \gg \varepsilon_1$ in the d-dimensional Q-state RGCL model with $\infty > d > 1$ and $Q > Q_0$.

It is obvious that the COP exists at $T = 0$ because $p_l = 1$ and $p_h = 0$. To prove the absence of the COP at $T \gg \varepsilon_1$, we begin with $T = \infty$, where $p_l = p_h = 1/2$. Before going to the proof, we outline its scenario. We first choose arbitrary one of the l-bond configurations in the COP. Let us denote it by $\mathscr{L}_l = (I_l, 1_l, 2_l, \ldots)$, assuming that only I_l become an infinite cluster for $N \to \infty$. In order to get a bond configuration of an h-bond percolated state to be compared with, we replace all the l-bonds except some in I_l by h-bonds, leaving all the finite clusters as they are. Then we calculate the number of all the possible spin configurations in a given restricted phase space for each of the pair of bond configurations, imposing the boundary condition that all the spins at the boundary of I_l are in a single spin state. We finally show that the relative probability of finding the COP vanishes for $N \to \infty$ compared with the h-bond percolated states.

Let us first concentrate our attention on I_l in $\mathscr{L}_l$ for $N < \infty$. When the boundary condition with a fixed spin state is given for the cluster, then this l-bond cluster can take only one spin configuration.

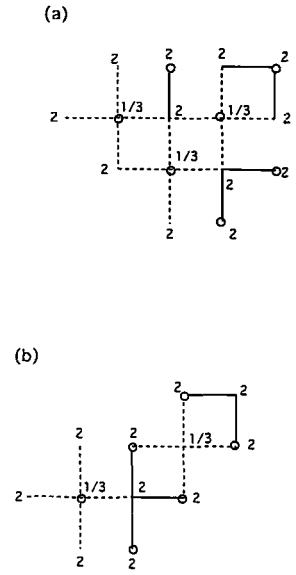

Fig. 5. Examples of h-bond configurations in bond graph I_l, solid and broken lines are l- and h-bonds; the boundary sites are fixed in a same spin state ($\sigma = 2$). (a) All the h-bonds form a single set, and the spin at every internal site of sublattice B (denoted by circles) can take states 1 and 3, while that in sublattice A is fixed in state 2. (b) The h-bonds is separated into two sets, and the assignment of spin states is made independently in each set so that the spin configurations are maximum.

Next we replace all the l-bonds in I_l by h-bonds except some l-bonds that have the boundary sites; the exclusion is made to satisfy the boundary condition. Then every internal site of I_l has z h-bonds except the one that has some of the nonreplaced l-bonds; here z is the coordination number of the lattice. Let us divide all the sites into two separate sublattices, as shown in Fig. 5. Having the boundary spins fixed in state 2, we count the number of possible spin states in the following two cases of bond configurations for which different restrictions to spin states are made. In one case where the h-bonds form a single nonseparated set as shown in Fig. 5(a), every spin in the A sublattice is kept in state 2 and the spins in the B sublattice can take states 1 and 3. In the other case where the h-bonds are separated into plural sets as shown in Fig. 5(b), we assign spin states independently in each cluster so that the number of spin configurations is the maximum. The number of sites that have two degrees of spin freedom is given in any case in the form

$$N_{\mathrm{I}} = \frac{2}{z}(b_{\mathrm{I}} - \Delta b_{\mathrm{I}}) \geqslant 0 \tag{4.2}$$

where Δb_1 is the correction caused by the boundary condition. Then the number of spin configurations in the replaced h-bond cluster of I_l subject to the fixed boundary condition is larger than or equal to $2^{N_1/2}$ in the restricted phase space.

Since the pair of bond configurations except I_l under the above boundary condition have the same number of spin configurations, the relative number of spin configurations for one bond configuration of the COP to the corresponding one of the percolated state subject to the restricted phase space is smaller than or equal to

$$2^{-N_1/2} \tag{4.3}$$

In the infinite cluster which is compact except at the phase transition point of second order, $\Delta b_1/b_1 = O(N^{-1+1/d})$ vanishes. Thus (4.3) vanishes for $N \to \infty$. In the same way we make the bond replacement for I_l of the other bond configurations of the COP. Then the above result holds true for any pair of bond configurations of the COP and the percolated state. Further removing the boundary condition and the restriction of phase space makes the percolated state favorable. Therefore there is no probability of finding the COP at $T = \infty$. Then one gets at least one h-bond percolated state from Theorem 2.

When $\varepsilon_1 = 0$, since $p_l = p_h = 1/2$, it is obvious that one has no COP at any temperature.

It is easy to extend the above proof to finite temperatures. Since the relative weight of the l-bond to the h-bond is $p_l/p_h = e^{K_1}$, it suffices to modify (4.3) by multiplying by $\exp(K_1 z N_1/2)$. Then at least one h-bond percolated state exists always above the temperature which satisfies $1/2\, e^{zK_1} < 1$, i.e., $T/\varepsilon_1 > z/\ln 2$.

5. PROOF OF THE PERCOLATED STATES IN THE GCL MODEL

We examine whether or not h-bond percolated states are stable at the presence of v-bonds. Based on Theorem 3, we give a proof of the following theorem in the simplest case of $\varepsilon_1 = 0$ (i.e., $p_l = p_h$) where no COP exists.

Theorem 4. Percolation of h-bonds occurs at $T \ll \varepsilon_2$ in the d-dimensional Q-state GCL model with $\varepsilon_1 = 0$ for $\infty > d > 1$ and $\infty > Q > Q_0$.

To this end we first define the v-bond cluster as the one made up of only neighboring v-bonds that possess a common site or are parallel to each other at the distance of the lattice constant. The v-bond clusters themselves have no meaning as connected objects, but they indicate separating l-bond clusters and h-bond clusters or making defects in these clusters. Thus, if there is no probability of percolation of v-bonds $[P_v(\infty) = 0]$,

it is certain that some ordered phase exists, though $P_v(\infty)>0$ is not a sufficient condition for the disorder to occur.

Let X be the coordinate of an arbitrary edge in the central part of the system and n_X the bond variable at X. We assume that the v-bond at X belongs to a v-bond cluster X_v which has b_X v-bonds, given $\tilde{n}$. Here X_v represents a graph. Then the bond graph $\mathscr{L}_v(\tilde{n})$ can be written as $\mathscr{L}_v=(X_v, \mathscr{L}_v^X)$, where $\mathscr{L}_v^X=(1_v, 2_v, \ldots)$ is the graph that consists of all the v-bond clusters except X_v in $\tilde{n}$. The probability of finding a v-bond at X that belongs to any cluster of size s is given by

$$P_v(s)=\sum_{\tilde{\sigma}} \sum_{\tilde{n}(\tilde{\sigma})} \mu(\tilde{n};\tilde{\sigma})\, \delta(b_X(\tilde{n}), s) \tag{5.1}$$

Using Eq. (3.13) and $p_l=p_h$, we write this in terms of clusters as

$$\begin{aligned} P_v(s)=&\frac{1}{Z_l}\sum_{\mathscr{L}_l} \sum_{\mathscr{L}_v\subseteq\mathscr{L}_{lc}} Q^{N_{1s}(\mathscr{L}_v)}\left(\frac{p_v}{p_l}\right)^{B_v(\mathscr{L}_v)} \delta(b_X, s) \\ &\times \prod_{\mu\in\mathscr{L}'_{uc}} \sum_{\tau_\mu} \prod_{\langle\mu\nu\rangle}{}^{\mathrm{i}}\, \delta(\tau_{\mu\nu}, 1) \end{aligned} \tag{5.2}$$

Here we have used $\sum_{\mathscr{L}_h\subseteq\mathscr{L}_{lc}}=\sum_{\mathscr{L}_v\subseteq\mathscr{L}_{lc}}$. Let us divide every quantity in $\mathscr{L}_v$ in Eq. (5.2) into two parts of X_v and $\mathscr{L}_v^X$. First the summation over $\mathscr{L}_v$ is separated as

$$\sum_{\mathscr{L}_v}=\sum_{\mathscr{L}_v^X}\sum_{X_v}' \tag{5.3}$$

where $\sum'_{X_u}$ is over X_v, while $\mathscr{L}_v^X$ is fixed. Then

$$B_v(\mathscr{L}_v)=B_v^X(\mathscr{L}_v^X)+b_X(X_v), \qquad N_{1s}(\mathscr{L}_v)=N_{1s}^X(\mathscr{L}_v^X)+n_{1s}(X_v) \tag{5.4}$$

where $B_v^X=B_v-b_X$, and N_{1s}^X and n_{1s} are the numbers of isolated one-site clusters in $\mathscr{L}_v^X$ and X_v, respectively. Then from Eqs. (5.1)–(5.4) and (3.13) one gets

$$\begin{aligned} P_v(s)=&\frac{1}{Z_l}\sum_{\mathscr{L}_l} \sum_{\mathscr{L}_v^X\subseteq\mathscr{L}_{lc}} Q^{N_{1s}^X}\left(\frac{p_v}{p_l}\right)^{B_v^X} \\ &\times\sum_{X_v}' Q^{n_{1s}}\left(\frac{p_v}{p_l}\right)^{b_X} \delta(b_X, s) \\ &\times \prod_{\mu\in\mathscr{L}'_{uc}} \sum_{\tau_\mu} \prod_{\langle\mu\nu\rangle}{}^{\mathrm{i}}\, \delta(\tau_{\mu\nu}, 1) \end{aligned} \tag{5.5}$$

Since isolated one-site clusters can exist only inside every v-bond cluster, one gets $n_{1s}(X_v) < 2b_X/z$. Then it is easy to get

$$\sum_{X_v}{}' Q^{n_{1s}(X_v)} \delta(b_X, s) < Q^{2s/z} \sum_{X_v}{}' \delta(b_X, s)$$
$$< Q^{2s/z} \sum_{X_v} \delta(b_X, s) \tag{5.6}$$

Note that the last sum in Eq. (5.6) is free from the restriction due to $\mathscr{L}_v^X$. Using $N_v^{\max}(s) \equiv \sum_{X_v} \delta(b_X, s)$, one gets

$$P_v(s) < \frac{1}{Z_l} \sum_{\mathscr{L}_l}^{X} \sum_{\mathscr{L}_v^X \subseteq \mathscr{L}_{lc}} Q^{N_{1s}^X} \left(\frac{p_v}{p_l}\right)^{B_v^X} \prod_{\mu \in \mathscr{L}'_{vc}} \sum_{\tau_\mu} \prod_{\langle \mu\nu \rangle}^{i} \delta(\tau_{\mu\nu}, 1)$$
$$\times Q^{2s/z} \left(\frac{p_v}{p_l}\right)^{s} N_v^{\max}(s) \tag{5.7}$$

Here $\sum_{\mathscr{L}_l}^X$ is the sum over l-bond graphs except those that include X. The degrees of bond freedom and spin freedom in X_v are taken out of the summation in the RHS of (5.7). Suppose we recover these degrees of freedom in the remaining and make all the possible bond configurations in X_v that consist only of l- and h-bonds. Let l_X be an arbitrary one of those l-bond graphs in X_v previously occupied by v-bonds. The number of those graphs is more than one for $s > 1$. Let $\mathscr{L}_{lX}$ denote an arbitrary one of the l-bond graphs (in $\mathscr{L}$) that include l_X. Then one gets $\sum_{\mathscr{L}_{lX}} > \sum_{\mathscr{L}_l}^X$ for $s > 1$. Then one gets the following inequality:

$$\frac{1}{Z_l} \sum_{\mathscr{L}_l}^{X} \sum_{\mathscr{L}_v^X \subseteq \mathscr{L}_{lc}} Q^{N_{1s}^X} \left(\frac{p_v}{p_l}\right)^{B_v^X} \prod_{\mu \in \mathscr{L}'_{vc}} \sum_{\tau_\mu} \prod_{\langle \mu\nu \rangle}^{i} \delta(\tau_{\mu\nu}, 1)$$
$$< \frac{1}{Z_l} \sum_{\mathscr{L}_{lX}} \sum_{\mathscr{L}_v \subseteq \mathscr{L}_{lXc}} Q^{N_{1s}} \left(\frac{p_v}{p_l}\right)^{B_v} \prod_{\mu \in \mathscr{L}'_{vc}} \sum_{\tau_\mu} \prod_{\langle \mu\nu \rangle}^{i} \delta(\tau_{\mu\nu}, 1)$$
$$= \frac{1}{Z_l} \sum_{\mathscr{L}_l} \sum_{\mathscr{L}_v \subseteq \mathscr{L}_{lc}} \left(\frac{p_v}{p_l}\right)^{B_v} \prod_{\mu \subseteq \mathscr{L}} \sum_{\tau_\mu} \prod_{\langle \mu\nu \rangle} \delta(\tau_{\mu\nu}, 1)$$
$$\times \prod_{\langle ij \rangle \in \mathscr{L}_v} \sum_{n_{ij}} [1 - \Delta(n_X, v)]$$
$$< 1 \tag{5.8}$$

where $\mathscr{L}_{lXc} = \mathscr{L} - \mathscr{L}_{lX}$. Note

$$\sum_{\mathscr{L}_v^X \subseteq \mathscr{L}_{lc}} = \sum_{\mathscr{L}_v \subseteq \mathscr{L}_{lXc}}$$

To get the third and fourth lines, we have used Eq. (3.13) and $\sum_{\tilde{\sigma}} \sum_{\tilde{n}} \mu(\tilde{n}; \tilde{\sigma}) = 1$, respectively. Then Eqs. (5.7) and (5.8) lead to

$$P_v(s) < Q^{2s/z} \left(\frac{p_v}{p_l} \right)^s N_v^{\max}(s) \tag{5.9}$$

It is easy to calculate the upper bound of $N_v^{\max}(s)$. Let us construct a cluster of size s by starting with a seed bond at X and putting bonds one by one on the constructing cluster. The second bond is put on one of the neighboring edges of the seed. Let z_v be the number of NN v-bonds that form a cluster, which is different from z. The third bond has $z_v - 1$ possible edges to proceed, but after that each bond does not necessarily have $z_v - 1$ possible edges. Thus, assuming that each bond has $z_v - 1$ possible edges to proceed, one is led to an overestimate of $N_v^{\max}(s)$ given by $z_v(z_v - 1)^{s-1}$; this includes also the overestimation that comes from different orders of construction and starting from different edges. Then one gets

$$P_v(s) < Q^{2s/z} z_v (z_v - 1)^{s-1} / (e^{K_2} - 1)^s \tag{5.10}$$

For $s \to \infty$ after taking the limit of $N \to \infty$, $P_v(s)$ becomes vanishing for $K_2 > \ln[1 + (z_v - 1) Q^{2/z}]$, and hence any h-bond percolated state is not destroyed. For the hypercubic lattice one has $z_v = 6$ in $d = 2$ and $z_v = 12$ in $d = 3$ because v-bond clusters have not only NN, but also NNN edges. Therefore, for $Q = 6$ there exists at least one h-bond percolated state always below $T/\varepsilon_2 \simeq 0.329$ in the simple cubic lattice and $T/\varepsilon_2 \simeq 0.387$ in the square lattice. Since both z and z_v depend on d, diverging for $d \to \infty$, thus the percolated state disappears for $d \to \infty$, and so for $Q \to \infty$. We note that $Q \to \infty$ does not lead to the ordinary plane rotator model in the present case.

6. COMPARISON WITH THE MONTE CARLO RESULTS IN $d = 3$

6.1. IOPs of the $Q = 6$ GCL Model

We have proved Theorem 4, but it can tell neither what color an h-bond percolated state has nor how many such states there are. However, making use of Theorem 4, we can obtain them from the numerical results of the six-state GCL model in the sc lattice previously obtained by the MC twist method.[13]

From Fig. 1, the IOP1 exists below $T/\varepsilon_2 \simeq 0.8$ at $\varepsilon_1 = 0$ in the sc lattice and is dominated by two adjacent states. In Section 5 at least one h-bond percolated state has been rigorously proved to exist always below $T/\varepsilon_2 \simeq 0.33$ at $\varepsilon_1 = 0$. From these results it follows that the IOP1 is the h-bond percolated state in one color.

At $\varepsilon_1 = 0$, the IOP2 is shown to exist at the intermediate temperatures between the IOP1 and the DP. Theorem 2 has revealed that if there are other phases than the DP and the COP, then they are all h-bond percolated states. Since it has clearly been shown in the MC study that the IOP2 is different from the COP and the DP, and is dominated by three adjacent spin states, then the IOP2 is also the h-bond percolated state in two adjacent colors.

From the last result it follows that the transition from the COP to the IOP2 is characterized only by the percolation of h-bonds in two adjacent colors; that is, it is topological without symmetry breaking. Thus we have verified the conjectures previously given by Ueno and Kasono.

6.2. Phase Diagram of the $Q=6$ GCL Model

We look at the qualitative properties of the phase boundaries of the IOPs from the percolation point of view. When one reduces p_h keeping $p_v \ll 1$ (or, almost equivalently, one changes ε_1, fixing T), the IOP1 should persist till some critical value of p_h/p_l ($\equiv r_{c1}$). This predicts $T_c(\text{IOP1} - \text{COP}) = \varepsilon_1 / \ln r_{c1}$. This is in good agreement with the MC result:

$$T_c(\text{IOP1} - \text{COP}) \simeq 3.40\varepsilon_1 \tag{6.1}$$

The coefficient in Eq. (6.1) gives $r_{c1} \simeq 0.745$, which is reasonable.

When one reduces p_h keeping p_h close to p_l (i.e., varying T), $T_c(\text{IOP1} - \text{IOP2})$ may be determined by some value of p_h/p_v ($\equiv r_{c2}$). This predicts $T_c(\text{IOP1} - \text{IOP2}) = (\varepsilon_2 - \varepsilon_1)/\ln(1 - r_{c2})$. This is in agreement with the MC result

$$T_c(\text{IOP1} - \text{IOP2}) \approx 1.2(1 - \varepsilon_1) \tag{6.2}$$

where $\varepsilon_2 = 1$ has been used. This gives a reasonable value of $r_{c2} \approx 1.3$.

Since the IOP2 made up of three different spin states tends to involve much more v-bonds than the IOP1, p_v should not be so small in the IOP2, which is consistent with the result obtained above ($p_v > p_h/1.3$). At the phase boundary between the IOP2 and DP, three kinds of bonds may be involved with about equal weight. In fact the boundary lies between two lines $T = 1/\log 2$ and $T = (1 - \varepsilon_1)/\log 2$ as shown in Fig. 1, which are obtained, respectively, from $p_l/p_v = 1$ and $p_h/p_v = 1$. It is remarkable that the critical point at $\varepsilon_1 = 0$ is very close to $1/\log 2 \simeq 1.44$, suggesting it is rigorous.

6.3. SOS Models in $d>2$

It has been revealed in Section 6.2 that the IOP2 needs v-bonds to exist. Then it cannot exist in the 3D RGCL model; namely, only the IOP1 can exist other than the COP. Thus the following theorem is suggested for the RSOS model in $d>2$ from Theorems 1 and 3.

Theorem 5. There exists only the h-bond percolated state of one color, namely the IOP1, other than the COP with the transition temperature less than $T/\varepsilon_1 = z/\ln 2$ in the d-dimensional RSOS model where $\infty > d > 2$.

In other words, the RSOS model undergoes the preroughening transition from the flat phase to the DOF phase of the IOP1 type. Let us confine ourselves to $d=3$ below. We can estimate this transition point making use of the result (6.1) obtained from the GCL model. When one approaches the RSOS model from the GCL model by taking the limit of $p_v \to 0$, there is another way, which takes $T \to 0$ and $\varepsilon_1 \to 0$ together keeping $K_1 = \varepsilon_1/T$ some constant and fixing $\varepsilon_2 = \varepsilon_3 = 1$, instead of the previous way, which takes $\varepsilon_2 = \varepsilon_3 \to \infty$ keeping T constant. Both ways lead to the same partition function so long as p_h/p_l $[= \exp(-K_1)]$ agrees in them. Then they give the same value of preroughening transition point $\varepsilon_1/T_{\rm pr}$, which becomes in the sc lattice

$$T_{\rm pr}/\varepsilon_1 \approx 3.40 \tag{6.3}$$

On the other hand, in the 3D discrete Gaussian model it has been proved that the surface tension is positive for $T>0$,[21] indicating the existence of a rigid phase (with $\psi = 2$), i.e., the flat phase. Thus no IOP is present for the $k=2$ model. Then one naturally expects there is a boundary k_c that separates SOS models in Eq. (4.1) into two: one phase transition in $k \geqslant k_c$ and no transition in $k < k_c$. One can approximately estimate k_c making use of Fig. 1. The SOS model is considered to show approximately the same behavior as the GCL model with $\varepsilon_2 = \varepsilon_3 = \varepsilon_1 2^k$ if $T \ll \varepsilon_2$. Let us consider it explicitly for $T/\varepsilon_2 < 0.1$. Then from Eq. (6.3) it follows that the model has a phase transition if $T_c/\varepsilon_2 = 3.4/2^k < 0.1$. Thus $k_c \simeq \ln 34/\ln 2 \approx 5.1$.

7. ORDER PARAMETERS OF THE PERCOLATED STATES

The novel type of percolated phases are characterized by nonzero percolation probabilities of l-bonds in color c, $P_{l\infty}^{(c)}$. We derive the expression of $P_{h\infty}^{(c)}$ by applying an infinitesimal field. Let us denote the h-bond colors by the unit vectors $\vec{C}(12),\ldots,\vec{C}(Q1)$ and let $\vec{C}(\sigma_i, \sigma_j) = (\cos\theta_{ij}, \sin\theta_{ij})$ be the variable of the h-bond color expressed in terms of spin variables. Let

us assume angle θ_{ij} takes $\pi(2q+1)/Q$ for color $c(qq+1)$. Then its explicit dependence on σ_i and σ_j is given by

$$\theta_{ij}=\begin{cases}(\pi/Q)(\sigma_i+\sigma_j) & \text{for} \quad |\sigma_i-\sigma_j|\neq Q-1\\ \pi/Q & \text{for} \quad |\sigma_i-\sigma_j|=Q-1\end{cases} \tag{7.1}$$

provided $n_{ij}=h$. We consider again our $Q=6$ GCL model and apply a fictitious external field $\vec{H}$ parallel to $\vec{C}(12)$ which acts on all the h-bonds uniformly,

$$\mathscr{H}_z(\tilde{n},\tilde{\sigma})=-\sum_{\langle ij\rangle}\vec{H}\cdot\vec{C}(\sigma_i,\sigma_j)\,\delta(\sigma_{ij},1)\,\Delta(n_{ij},h) \tag{7.2}$$

Then p_h depends on $\vec{H}\cdot\vec{C}(\sigma_i,\sigma_j)$ and thus is replaced in Eqs. (3.4) and (3.8) by

$$p_h(\vec{H}\cdot\vec{C}_{ij})=[\exp(-K_1+\beta\vec{H}\cdot\vec{C}_{ij})-\exp(-K_2)]/A(\vec{H}\cdot\vec{C}_{ij}) \tag{7.3}$$

where $A(\vec{H}\cdot\vec{C}_{ij})=p_l+p_h(\vec{H}\cdot\vec{C}_{ij})+p_v$. Here $\vec{C}_{ij}$ is the abbreviation for $\vec{C}(\sigma_i,\sigma_j)$. Then instead of Eq. (3.9b) we get

$$\mu(\tilde{n};\tilde{\sigma})=\frac{1}{Z_v}\left(\frac{p_l}{p_v}\right)^{B_l(\tilde{n}_0)}\prod_{\langle ij\rangle\in\mathscr{L}_h}\frac{1}{p_v}p_h(\vec{H}\cdot\vec{C}_{ij}) \tag{7.4}$$

The probability of infinite clusters of h-bonds in $\vec{C}(12)$ is given by

$$P_{h\infty}^{(12)}=\lim_{H\to 0}\lim_{N\to\infty}\frac{1}{E}\frac{\partial}{\partial\beta H}[\ln Z(H)] \tag{7.5}$$

as verified below, where $E=zN/2$ for $N\to\infty$. Using Eqs. (7.4) and (3.13), one gets

$$\begin{aligned}P_{h\infty}^{(12)}&=\lim_{H\to 0}\lim_{N\to\infty}\frac{1}{Z_v}\sum_{\tilde{\sigma}}\sum_{\tilde{n}(\tilde{\sigma})}\left(\frac{p_l}{p_v}\right)^{B_l}\\&\quad\times\prod_{\langle ij\rangle\in\mathscr{L}_h}\frac{1}{p_v}p_h(\vec{H}\cdot\vec{C}_{ij})\frac{1}{E}\sum_{\langle ij\rangle\in\mathscr{L}_h}\vec{C}(12)\cdot\vec{C}_{ij}\\&=\lim_{H\to 0}\lim_{N\to\infty}\frac{1}{Z_v}\sum_{\mathscr{L}_l}\sum_{\mathscr{L}_h\subseteq\mathscr{L}_{lc}}\prod_{\mu\in\mathscr{L}_l}\left(\frac{p_l}{p_v}\right)^{b_\mu}Q^{N_{1s}(\mathscr{L}_v)}\\&\quad\times\prod_{\mu\in\mathscr{L}'_{vc}}\sum_{\tau_\mu}\prod_{\langle\mu\nu\rangle}{}^{\mathrm{i}}\,\delta(\tau_{\mu\nu},1)\\&\quad\times\prod_{\xi\in\mathscr{L}_h}\left[\frac{p_h}{p_v}+[\exp(K_2-K_1)](\exp[\beta\vec{H}\cdot\vec{C}_\xi(\tau_\mu,\tau_\nu)]-1)\right]^{b_\xi(\mathscr{L}_h)}\\&\quad\times\frac{1}{E}\sum_{\xi\in\mathscr{L}_h}b_\xi(\mathscr{L}_h)\,\vec{C}(12)\cdot\vec{C}_\xi(\tau_\mu,\tau_\nu)\end{aligned} \tag{7.6}$$

where $\vec{C}_\xi(\tau_\mu, \tau_\nu)$ is the color of the ξth h-bond cluster which connects the μth and νth l-bond clusters. The contribution of finite clusters in $N \to \infty$ vanishes as $H \to 0$ because the field does not work to select clusters in $\vec{C}(12)$ and the sum of $\vec{C}_\xi(\tau_\mu, \tau_\nu)$ vanishes when the relevant joint cluster takes all the spin states. On the other hand, when one compares the probability of infinite clusters in $\vec{C}(12)$ with that of those in colors different from $\vec{C}(12)$, an infinite cluster (or clusters) in $\vec{C}(12)$ survives because the relative probability of the latter to the former vanishes as

$$\lim_{H \to 0} \lim_{N \to \infty} \left[\frac{\exp(-K_1 + \beta \vec{H} \cdot \vec{C}_\xi) - \exp(-K_2)}{\exp(-K_1 + \beta H) - \exp(-K_2)} \right]^{b_\xi(\mathscr{L}_h)} \to 0$$

Then one is led to

$$\begin{aligned} P_{h\infty}^{(12)} &= \lim_{N \to \infty} \frac{1}{Z_{N,v}} \sum_{\tilde{\sigma}} \sum_{\tilde{n}(\tilde{\sigma})} \left(\frac{p_l}{p_v} \right)^{B_l(\tilde{n}_0)} \left(\frac{p_h}{p_v} \right)^{B_h(\tilde{n}_1)} \\ &\quad \times \frac{1}{E} \sum_{\xi \in \mathscr{L}_h}^{*} b_\xi(\mathscr{L}_h)\, \delta(\vec{C}_\xi(\tilde{\sigma}), \vec{C}(12)) \\ &= \lim_{N \to \infty} \frac{1}{QE} \left\langle \sum_{\xi \in \mathscr{L}_h}^{*} b_\xi(\mathscr{L}_h) \right\rangle_{n\sigma} \end{aligned} \tag{7.7}$$

where $\sum_\xi^*$ is the sum over infinite h-bond clusters and $\langle \cdots \rangle_{n\sigma}$ the average with respect to $\mu(\tilde{n}; \tilde{\sigma})$.

Even when one gets $P_{h\infty}^{(12)} > 0$, one cannot determine in what color state the phase is. To investigate it, we apply external fields in more than one direction with the same strength. For instance, suppose one applies two fields in $\vec{C}(12)$ and $\vec{C}(23)$, and measures $P_{h\infty}^{(12)}$ and $P_{h\infty}^{(23)}$. In the case where only one of them is nonvanishing one gets an IOP1. Otherwise there occurs percolation of h-bonds whose colors are equal to or more than two in number. Then one has to increase more fields which orient in more directions.

Further fluctuations of the IOPs are measured by the susceptibility

$$\Xi_h = \lim_{N \to \infty} E\langle \Delta P_{h\infty}^{(c)}\, \Delta P_{h\infty}^{(c)} \rangle \tag{7.8}$$

where $\Delta P_{h\infty}^{(c)} = P_{h\infty}^{(c)} - \langle P_{h\infty}^{(c)} \rangle$.

8. ALGORITHM IN TERMS OF CLUSTERS

It is useful first to see how thermal fluctuations appear in our description. Although they generate v- and h-bonds, it is convenient to regard

them as generating only v-bonds, as shown below; this may be a viewpoint from the ordered world. Then they appear in two ways, as simply seen in the following expression of the partition function:

$$Z = A^E \sum_{\tilde{\sigma}} (p_l + p_v)^{E_0(\tilde{n}_0)} (p_h + p_v)^{E_1(\tilde{n}_1)} p_v^{E_c(\tilde{n}_c)} \tag{8.1}$$

In the first, v-bonds appear in $\tilde{\sigma}$ for $\sigma_{ij} \neq 0, 1$, as seen in the last factor of this equation. In the second, they appear in $\tilde{n}$ for l- and h-bonds with relative probabilities p_v/p_l and p_v/p_h, respectively.

We propose a cluster algorithm of MC simulations for the GCL model based on the present description. In the first step, specify $\mathscr{L}_0$ and $\mathscr{L}_1$ after $\tilde{\sigma}$ is given. Then determine a bond state $\tilde{n}$ by generating v-bonds in $\mathscr{L}_0$ with probability $p_v/(p_l + p_v)$ and in $\mathscr{L}_1$ with $p_v/(p_h + p_v)$, apart from the v-bonds automatically given for $\sigma_{ij} \neq 0, 1$. Then specify the l- and h-bond clusters $\{\mu_l\}$, $\{\xi_h\}$ from $\tilde{n}$ and the cluster spins $\{\tau_\mu\}$ including the one-site cluster spins from $\tilde{\sigma}$.

In the next step, update $\{\tau_\mu\}$ to get a new spin state $\{\tau'_\mu\}$ by taking into account their interactions determined by ξ_h. To this end let us introduce cluster spins $\{S_\omega\}$ of the joint clusters $\{\omega_{jc}\}$ defined in Section 3.4; here S_ω is defined by some reference direction of all the spins in a joint cluster with their relative spin directions $\{\Delta\tau\}$ being fixed, $\{\tau_\mu\} = \{\Delta\tau_\mu + S_\omega;\ \mu \in \omega_{jc}\}$. Then the next step is equivalent to updating $\{S_\omega\}$ independently to get a new spin state $\tilde{\sigma}' = \{\tau'_\mu\}$. Then return the first step and keep repeating this process.

There is a variation of the above algorithm. This treats the system as interacting l-bond clusters by eliminating h- and v-bonds. To this end we derive below the expression of Z written in terms of only l-bond clusters. Using Eq. (3.4), one gets

$$\begin{aligned} Z &= A^E \sum_{\tilde{\sigma}} \sum_{\tilde{n}} \prod_{\langle ij \rangle \in \mathscr{L}_l} p_l \delta(\sigma_{ij}, 0) \\ &\quad \times \prod_{\langle ij \rangle \in \mathscr{L}_{lc}} \sum_{n_{ij} \neq l} \{ p_h \delta(\sigma_{ij}, 1)\, \Delta(n_{ij}, h) + p_v \Delta(n_{ij}, v) \} \\ &= A^E \sum_{\mathscr{L}_l} \prod_{i \in \mathscr{L}_l} \sum_{\sigma_i} \prod_{\langle ij \rangle \in \mathscr{L}_l} p_l \delta(\sigma_{ij}, 0) \\ &\quad \times \prod_{i \in \mathscr{L}_c} \sum_{\sigma_i} \prod_{\langle ij \rangle \in \mathscr{L}_{lc}} (p_h \delta(\sigma_{ij}, 1) + p_v) \end{aligned} \tag{8.2}$$

Then this is written in terms of l-bond clusters as

$$Z = (A p_v)^E \sum_{\mathscr{L}_l} \prod_{\mu \in \mathscr{L}_l} \left(\frac{p_l}{p_v} \right)^{b_\mu} \sum_{\tau_\mu} \prod_{\mu \in \mathscr{L}_{lc}} \sum_{\tau_\mu} \prod_{\langle \mu\nu \rangle} e^{(K_2 - K_1) S_{\mu\nu}} \delta(\tau_{\mu\nu}, 1) \tag{8.3}$$

where $S_{\mu\nu}$ is the number of edges whose sites belong to the μth and νth clusters.

In the first step, after having specified $\mathscr{L}_0$ given $\tilde{\sigma}$, determine one of the l-bond configurations in $\mathscr{L}_0$ (which forms a lattice graph $\mathscr{L}_l$) by generating each l-bond with probability $p_l/(p_l+p_v)$. Then specify the clusters including the one-site clusters together with cluster spins $\{\tau_\mu\}$ and calculate $\{S_{\mu\nu}\}$. In the next step, making use of the measure in Eq. (8.3), perform the standard MC simulation for the interacting cluster system given by $\{\tau_\mu\}$ and $\{S_{\mu\nu}\}$, for an appropriate time. After getting in thermal equilibrium by repeating this process, save a considerable amount of data on $\mathscr{L}_l$. Then one can get data on $\mathscr{L}_h$ from them by using the first step of the first algorithm.

9. COMMENTS ON RELATED MODELS

9.1. Comments on the GCL and RSOS Models in Two Dimensions

In the 2D GCL model including the ordinary one, it has been established that the model has an intermediate phase of the KT type for $Q>4$ and this phase is equivalent to the rough phase.[15,19] Thus this is an h-bond percolated state with the full color symmetry of h-bonds, as shown in Section 4.

Recently Rommelse and den Nijs studied the RSOS model with NNN interactions on the square lattice and found a novel type of intermediate phase called the disordered flat (DOF) phase.[22] In this phase only two adjacent heights are dominant. From Theorem 2, it is certain that steps in one color are percolated, i.e., the DOF phase is the IOP1 in $d=2$. This is attributed to the NNN interactions because they couple step contours of the same color.[22]

This phase is also of considerable interest from another point of view: it is equivalent to the Haldane phase in the corresponding $S=1$ antiferromagnetic quantum chain; in this phase the excitation spectrum has a (Haldane) gap.[23] Tasaki already proposed a percolation picture of phase transitions in the same quantum model.[24]

Recently Shioda and Ueno studied the $Q=6$ GCL model with NNN interactions by the twist method, employing relatively large-scale Monte Carlo simulations.[25] The interactions of the model are given by

$$V_1(\sigma_{ij}) = \varepsilon_{\mathrm{n1}}\delta(\sigma_{ij},1) + \varepsilon_{\mathrm{n2}}[\delta(\sigma_{ij},2)+\delta(\sigma_{ij},3)]$$

$$V_2(\sigma_{kl}) = \varepsilon_{\mathrm{nn}}[\delta(\sigma_{kl},2)+\delta(\sigma_{kl},3)]$$

with $0 < \varepsilon_{n1} < \varepsilon_{n2}$ and $\varepsilon_{nn} > 0$ for NN and NNN interactions, respectively. The phase diagram of T versus ε_{n1} with $\varepsilon_{n2} = \varepsilon_{nn} = 2.0$ is quite similar to that of the 3D GCL model[13] and also of the RSOS model,[22,26] within the range of calculations ($0 \leqslant \varepsilon_{n1} < 1.6$). Shioda and Ueno found an IOP2 with $\psi \approx 0.1$, but neither IOP1 nor the rough phase, though they cannot be ruled out in a narrow region at very low temperatures.

To get the RSOS model from the GCL model, we take the limit of p_v $[\propto \exp(-\varepsilon_{n2}/T)] \to 0$ in the same way as done in Section 6 for the 3D models. However, since the NNN energy parameter ε_{nn} is kept fixed, one is led to the RSOS model with the infinite NNN interaction. From the result of the GCL model the preroughening temperature for $\varepsilon_{nn} = \infty$ is estimated as

$$T_{pr}/\varepsilon_{n1} \approx 1.55 \tag{9.1}$$

This is quite consistent with the phase diagram of the RSOS model.[22]

9.2. Comment on the Chiral Clock Model

It is interesting to consider the chiral clock model[27] for a comparison with the GCL model. We estimate the stiffness exponent ψ of the incommensurate (IC) phases, making use of the results obtained previously. The Hamiltonian of this model on the simple square and cubic lattices is given as

$$H = -\sum_{\langle ij \rangle} \cos \frac{2\pi}{Q} (\sigma_i - \sigma_j - \vec{\Delta} \cdot \hat{x}_{ij}) \tag{9.2}$$

where $\vec{\Delta} = \Delta \hat{x}$ for $0 < \Delta < 0.5$ ($\hat{x}$ is a unit lattice vector) and $\hat{x}_{ij}$ is the unit vector directing from site i to j in a nearest neighbor. At $\Delta = 0.5$, the degree of ground-state degeneracy is highest, but its entropy is vanishing, $O(L^{1-d})$, whereas $S = O(L^0)$ in the GCL model at $\varepsilon_1 = 0$. As is well known, the IC phase is well described by an array of extended domain walls perpendicular to $\vec{\Delta}$; the phase of each domain is rotating with a wave vector $\vec{q} \parallel \vec{\Delta}$.

In $d = 2$, the domain walls in the IC phase are floating with no long-range order. Using the free energy $F_n(T, L)$ of the untwisted system with average wall number n obtained in the free fermion approximation,[26] it is easy to calculate the stiffness exponent. We give only the result for the stiffness free energy for $Q > 2$,

$$\Delta F(T, L) \equiv F_{n+1}(T, L) - F_n(T, L) = O(L^0)$$

Thus, one gets $\psi = 0$ as expected, indicating the IC phase is a critical state.

In $d=3$, similarly one can estimate ψ, making use of a phenomenological free energy for a given mean wall separation $l=L/n$.[28] Then one gets the stiffness free energy for the increase of one wall for $Q \geqslant 6$, $\Delta F = O(L)$. Therefore one gets $\psi = 1$, which indicates the XY-like behavior. However at $\Delta = 0$, that is, in the ordinary clock model, Ueno and Mitsubo found the IOP1 at intermediate temperatures by the MC twist method,[12] against theoretical expectation.[28] Because of thermal fluctuations, this IOP1 is expected to extend to some finite value of Δ and have a phase boundary with the IC phase. It is reasonable that both phases are different in view of the extreme difference in the degrees of degeneracy.

10. DISCUSSIONS OF IOPS

10.1. Interactions Between Random Surfaces of h-Bonds

There is competing or frustration in interactions via h-bonds among l-bond clusters in certain kinds of configurations. Since clusters are variable in shape and size, there are many configurations such that only three l-bond clusters are close to each other: clusters D, C, E in Fig. 6. Then all of them cannot be connected by h-bonds, because three different pairs among the clusters cannot be all $\tau_{\mu\nu}=1$. They are competing.

This property can be put in another way, i.e., as interactions between h-bond surfaces. Suppose three l-bond layers are formed and neighboring layers are separated by h-bond surfaces. Let them be in states 1, 2, and 3. Further suppose part of the outer layers push out the internal one and get in touch with each other. Then the above competing effect between l-bond layers works as repulsive interactions between neighboring h-bond surfaces in different colors $c(12)$, $c(23)$. On the other hand, when the spin states of

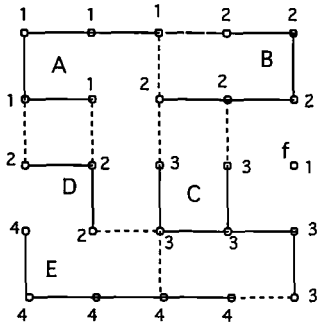

Fig. 6. Bond and spin configurations which bring about competing interactions among three l-bond clusters denoted by C, D, and E.

the layers are 1, 2, and 1, there is no such an effect. Thus one can regard that the surfaces in the same color $c(12)$ have attrative interactions from a relative point of view. Therefore the IOP1 is preferred to the IOP2 and others in $d=3$. However, as temperature gets higher (or p_v increases) the competing effect becomes weak enough to allow the IOP2 to appear. The strength of these effective interactions seems to depend strongly on dimension; it is stronger in $d=3$ than in $d=2$.

10.2. Large-Entropy Contribution

Entropy contribution is considered indispensable to the occurrence of the IOPs. As one sees in the proof of Theorem 3, the number of spin configurations in the h-bond percolated state is overwhelming compared with the COP even if the phase space is limited; this requires $p_h \sim p_l$ or $T \gg \varepsilon_1$. Also indispensable is the energy barrier with height ε_2 that protects the IOPs from v-bonds, i.e., getting disordered; this is effective till p_v is close to 1 or T is close to ε_2, from the result in Section 6.2.

Let us estimate the average number of h-bonds in the IOP1 at $\varepsilon_1=0$ of the GCL model in the sc lattice when $p_v \ll 1$. Then we can approximate that the IOP1 consists only of l- and h-bonds and the l-bond clusters are only in two colors, say $c(1)$ and $c(2)$. Then this is the random site percolation problem in $d=3$ with concentration $p=0.5$. Thus the numbers of bonds are $B_l=B_h=\frac{1}{2}E=\frac{3}{2}N$. Since $p_c \simeq 0.311 < p=0.5 < 1-p_c$,[1] two infinite clusters of both colors can coexist, so that h-bonds between them are necessarily percolated.

Since p is not close to p_c, most of the l-bonds belong to either of the infinite clusters. Then most of the h-bonds connect those l-bonds which belong to different infinite clusters. Although h-bonds form surfaces, their number is extremely large. Therefore we conclude that the surface of the infinite cluster of h-bonds is extremely crumpled and wrinkled with fractal dimensions $d_f=3$. Such configurations of the surfaces yield large entropy. Thus we consider the IOP1 is the order due to entropy gain.[8,13,29] We also consider the IOP2 to be so.

10.3. Excitations and the Stiffness Exponent

The MC study[12,13] has revealed that the excitations in the IOPs have a peculiar structure, which is closely related to the nonintegral stiffness exponent. Let us confine ourselves to the IOP1 of the GCL model. Suppose the IOP1 consists of infinite clusters of states 2 and 3, i.e., colors $c(2)$ and $c(3)$, and an l-bond cluster in $c(1)$ is excited in the infinite cluster of color $c(2)$. This finite cluster is confined almost within this infinite cluster. Since

there are strong repulsive interactions between h-bond surfaces of different colors as already discussed, it can hardly get in touch with another infinite cluster. In this sense excitations are protected by buffers of h-bond surfaces which surround them. If the linear size L_{ex} of an excited cluster is large enough, then the interaction energy becomes about $\varepsilon_2 L_{ex}^{\psi}$. Here ε_1 is irrelevant because its effect is lost by thermal fluctuations, as verified by the fact that there is no stiffness for the lowest twist angle $\phi = \pi/3$ (as given in Section 2). The present explanation is consistent with the profiles of the twisted system.[12,13] Similar excitations are also expected in the IOP2.

10.4. Nonlocal Character of the Order Parameters

It is worth pointing out a remarkable property of the order parameters of the IOPs. Percolating quantities are of nonlocal character, in the sense that one cannot determine locally whether the percolation of the element of interest occurs or not. In particular, this character becomes important in the case that the onset of percolation does not break the macroscopic symmetry of the system, i.e., symmetry of l-bond colors. The transition between the IOP2 and the COP is such a case, as already explained in Section 6. Then one has no means to observe the order parameter directly unless one could manage to generate a field in Eq. (7.2).

This remarkable property has already been known for the den Nijs–Rommelse order paraeter[22] of the Haldane phase in the $S=1$ AF quantum Heisenberg chain.[23] It is no wonder, because this model is a quantum version of the RSOS model with NNN interactions and the Haldane phase corresponds to the DOF phase which is of the IOP1 type, as discussed in Section 9.

10.5. Universal Behavior of the IOPs

The IOPs have already been found in other $d=3$ models, such as the AF Potts models, a stacked triangular AF Ising model, and a stacked square frustrated Ising model, including the ordinary $Q=6$ clock model. Details are summarized in ref. 13. For the models whose order parameter space of the COP is plane ($d_{op}=2$), the stiffness exponents of these IOPs are close to $\psi \simeq 1.2$, much smaller than $\psi = 2$ of the COP, but clearly larger than $\psi = 1$ for the XY model. On the other hand, the other models with different values of d_{op} have different values of the stiffness exponent: $\psi \simeq 1.8$ and 0.7 for $d_{op}=3$ and 4, respectively.[8] Thus these values suggest universality.

10.6. Critical Properties

It is natural to expect distinct critical properties because the IOPs are essentially different from the known ordered phases even if the topological transition between IOP2 and COP is put aside. There are some numerical calculations and experiments of critical exponents. In our description the phase transitions studied in them are all those between disorder and IOP1 or IOP2. For the $Q=3$ AF Potts model where only the IOP1 was observed, Ueno *et al.*[8] obtained the following values:

$$\nu = 0.58 \pm 0.01, \qquad \beta = 0.34 \pm 0.02, \qquad \gamma = 1.10 \pm 0.02$$

with $T_c = 1.235 \pm 0.005$. They also obtained $\alpha = 0.15$, which is much less accurate. For the same model, Wang *et al.*[9] obtained

$$\nu = 0.66 \pm 0.03, \qquad \gamma = 1.31 \pm 0.09$$

with $T_c = 1.2259 \pm 0.0007$. They are close to those of the XY universality class ($\nu = 0.669$, $\beta = 0.346$, $\gamma = 1.316$).[30] Others also studied such models with Z_6 symmetry to get estimates close to these.[31] The differences between both sets of values are so large that it is difficult to attribute them to the error of T_c in the former.[9] Rather, it is reasonable to attribute them to whether or not the anisotropy has been manifest and thus effective in the calculations. In the former study it was clearly observed below T_c in the same manner as shown in Section 2 for the GCL model, and the estimations were done there. On the other hand, in the latter, the calculations were done in the region where the anisotropy is lost, although they observed it fairly below T_c.

Recently Ajiro *et al.* and Kadowaki *et al.* performed experiments on $CsMnI_3$, which undergoes two phase transitions.[32,33] Both are considered equivalent to the systems with Z_6 symmetry. They obtained

$$\nu = 0.59 \pm 0.03, \qquad \beta = 0.32 \pm 0.01, \qquad \gamma = 1.12 \pm 0.07$$

$$\nu = 0.56 \pm 0.02, \qquad \beta = 0.35 \pm 0.01, \qquad \gamma = 1.04 \pm 0.03$$

for the higher and lower transitions ($T_c = 11.2$, 8.2 K), respectively. They are in good agreement with the values obtained by Ueno *et al.*[8] within the errors of each study, obviously different from those of the XY class.

Some exponents were also calculated for other models by the MC twist method as follows. The stacked triangular AF Ising model in $d=3$ undergoes a phase transition from IOP2 to disorder at $T_c \simeq 3.64$, $\nu = 0.57 \pm 0.03$, and $\alpha = 0.21$.[11] The $Q=6$ clock model has a phase transition at $T_c \simeq 3.04$ (in the stacked triangular lattice) between IOP1 and

disorder; $\nu = 0.57 \pm 0.03$ and $\alpha = 0.18$.[12] Though the values of α are much less accurate, they are consistent with hyperscaling, $d\nu = 2 - \alpha$.

The results obtained rigorously in Section 6 together with those of the stiffness exponent are strong evidence against the XY universality class. This is because they rule out order of XY character, which should have $\psi = 1$ for any twist angle; in other words, IOP1 and IOP2 should be degenerate with each other.

11. SUMMARY

Introducing physical connections and disconnections, we have formulated a new description of the GCL model in terms of them. Based on the description, we have proved that the IOPs found by the MC studies are a novel type of percolated state, by the following procedure.

We introduced PC-type models with discrete single-valued variables and proved that only COP and/or h-bond percolated state(s) are possible to exist in these models (Theorem 2). For the RGCL model, which is one of the restricted models of PC type (Theorem 1), we proved on the basis of Theorem 2 that it has the COP and at least one h-bond percolated state at lower and higher temperatures, respectively, in a large range of d and Q (Theorem 3). In the simplest case ($\varepsilon_1 = 0$) of the GCL model, we proved on the basis of Theorem 3 that percolation of h-bonds occurs at low temperature in the same range of d and Q as for Theorem 3 (Theorem 4). From Theorem 4 and the MC results, we verified the previous conjectures on a simple version of the six-state GCL model in $d = 3$ that the IOP1 and IOP are h-bond percolated states of one color and two adjacent colors, respectively, and that the transition between the COP and IOP2 is characterized only by h-bond percolation. We also succeeded in explaining the phase diagram of the same model obtained by the MC twist method, in terms of bond percolation.

The present description connects the RSOS and GCL models in a certain limit. Using this relation, we estimated the preroughening temperature in $d = 3$ to be $T_{\rm pr} \simeq 3.40\varepsilon_1$. Further, it follows from the results on the IOP1 and IOP2 obtained in Section 6 that only the IOP1 other than the COP exists in the RSOS model for finite $d > 2$ and $Q > Q_0$ (Theorem 5).

Finally, we note some important aspects of the present study.

1. Genuine local forces (i.e., l- and h-bond variables) are newly introduced degrees of freedom, namely, hidden variables. Although the quantity of percolated l-bonds is given by magnetization, that of percolated h-bonds is completely hidden (though the onset may be detected through magnetization); that is, the IOPs are hidden orders. It is the symetry of the topological partition of the system that is relevant to the hidden orders.

2. The rough phase may be regarded as a special case of the IOPs, namely, as a percolated state of surfaces where interactions between surfaces are insufficient.

3. One cannot directly observe h-bonds, thus percolation of h-bonds. It is surprising and might be very important to recognize that there can be orders that cannot be observed directly. A good substitute for it is the stiffness amplitude $A(T)$ of the stiffness free energy with a nonintegral value of exponent. This quantity seems very difficult but possible in principle to observe.

4. The present approach from local force has been shown to be more fundamental than that from the order parameter in a general case of models with discrete symmetry.

ACKNOWLEDGMENTS

The author would like to thank P. Nightingale, M. Fisher, and D. Sherrington for useful discussions and hospitality. He is also grateful to D. Hamuro, T. Inoue, T. Satomura, H. Shioda, K. Kasono, A. Yamagata, Y. Ozeki, Y. Taguchi, and I. Ono for stimulating discussions. He also thanks P. Erdősh for giving a copy of the lecture notes in ref. 5. This work was partly supported by Grant-in-Aid for Scientific Research on Priority Areas, Computational Physics as a New Frontier in Condensed Matter Research, under grant no. 03247212 from the Ministry of Education, Science and Culture.

REFERENCES

1. D. Stauffer, *Phys. Rep.* **54**:1–74 (1979).
2. P. W. Kasteleyn and C. M. Fortuin, *J. Phys. Soc. Jpn.* **26**(suppl.):11 (1969); *Physica* **57**:536 (1972).
3. A. Coniglio and W. Klein, *J. Phys. A* **13**:2775 (1980); C.-K. Hu, *Phys. Rev. B* **29**:5103 (1984); C.-K. Hu and C.-N. Chen, *Phys. Rev. B* **38**:2765 (1988).
4. R. H. Swendsen and J.-S. Wang, *Phys. Rev. Lett.* **58**:86 (1987).
5. R. G. Edwards and A. D. Sokal, *Phys. Rev. D* **38**:2009 (1988); A. D. Sokal, Monte Carlo methods in statistical mechanics: Foundations and algorithms, Lecture Notes, Troisième Cycle de la Physique en Suisse Romande (1989).
6. M. D. De Meo, D. W. Heermann, and K. Binder, *J. Stat. Phys.* **60**:585 (1990).
7. A. N. Berker and L. P. Kadanoff, *J. Phys. A* **13**:L259 (1980); J. Banavar, G. S. Grest, and D. Jasnow, *Phys. Rev. B* **25**:4639 (1982); I. Ono, *Prog. Theor. Phys. Suppl.* **87**:102 (1986).
8. Y. Ueno, G. Sun, and I. Ono, *J. Phys. Soc. Jpn.* **58**:1162 (1989); Errata, *J. Phys. Soc. Jpn.* **61**:4672 (1992).
9. J.-S. Wang, R. H. Swendsen, and R. Kotecký, *Phys. Rev. B* **42**:2465 (1990).
10. M. Mekata, *J. Phys. Soc. Jpn.* **42**:76 (1977); F. Matsubara and S. Inawashiro, *J. Phys. Soc. Jpn.* **53**:4373 (1984); D. Blanckschtein, M. Ma, and A. Berker, *Phys. Rev. B* **29**:5250 (1984).

11. K. Mitsubo, G. Sun, and Y. Ueno, in *Cooperative Dynamics in Complex Systems*, H. Takayama, ed. (Springer, Berlin, 1989), p. 49; K. Mitsubo and Y. Ueno, Unpublished.
12. Y. Ueno and K. Mitsubo, *Phys. Rev. B* **43**:8654 (1991); P. D. Scholten and L. J. Irakliotis, *Phys. Rev. B* **48**:1291 (1993).
13. Y. Ueno and K. Kasono, *Phys. Rev. B* **48**:16471 (1993).
14. O. Nagai, Y. Yamada, and H. T. Diep, *Phys. Rev. B* **32**:480 (1985); G. Sun and Y. Ueno, *Z. Phys.* **82**:425 (1991).
15. J. L. Cardy, *J. Phys. A* **13**:1507 (1980).
16. H. Shioda and Y. Ueno, *J. Phys. Soc. Jpn.* **62**:970 (1993).
17. J. D. Weeks, in *Ordering in Strongly Fluctuating Condensed Matter Systems*, T. Riste, ed. (Plenum Press, New York, 1980), p. 293.
18. M. den Nijs, *J. Phys. A* **18**:L549 (1985).
19. S. T. Chui and J. D. Weeks, *Phys. Rev. B* **14**:4978 (1976); H. J. F. Knops, *Phys. Rev. Lett.* **39**:766 (1977); J. V. José, L. P. Kadanoff, S. Kirkpatrick, and D. R. Nelson, *Phys. Rev. B* **16**:1217 (1977).
20. J. M. Kosterlitz and D. J. Thouless, *J. Phys. C* **6**:1181 (1973); J. M. Kosterlitz, *J. Phys. C* **7**:1047 (1974).
21. M. Göpfert and G. Mack, *Commun. Math. Phys.* **82**:545 (1982).
22. K. Rommelse and M. den Nijs, *Phys. Rev. Lett.* **59**:2578 (1987).
23. F. D. M. Haldane, *Phys. Lett.* **93A**:464 (1983); *Phys. Rev. Lett.* **50**:1153 (1983); M. den Nijs and K. Rommelse, *Phys. Rev. B* **40**:4709 (1989).
24. H. Tasaki, *Phys. Rev. Lett.* **66**:798 (1991).
25. H. Shioda and Y. Ueno, *J. Phys. Soc. Jpn.* **62**:4224 (1993).
26. D. Hamuro, Y. Ueno, and G. Sun, unpublished.
27. S. Ostlund, *Phys. Rev. B* **24**:398 (1981).
28. M. E. Fisher and D. S. Fisher, *Phys. Rev. B* **25**:239 (1982); O. A. Huse and M. E. Fisher, *Phys. Rev. B* **29**:239 (1984).
29. Y. Ueno, *J. Phys. Soc. Jpn.* **55**:2586 (1986); G. Sun, Y. Ueno, and Y. Ozeki, *J. Phys. Soc. Jpn.* **57**:156 (1988).
30. J. C. Le Guillon and J. Zinn-Justin, *Phys. Rev. B* **21**:3976 (1980).
31. T. Ohyama and H. Shiba, *J. Phys. Soc. Jpn.* **61**:4174 (1992); Y. Okabe and M. Kikuchi, Unpublished.
32. Y. Ajiro, T. Inami, and H. Kadowaki, *J. Phys. Soc. Jpn.* **59**:4142 (1990).
33. H. Kadowaki, T. Inami, Y. Ajiro, and Y. Endoh, *J. Phys. Soc. Jpn.* **60**:1708 (1991).